XII International Conference on Computational Plasticity. Fundamentals and Applications
COMPLASS XII
E. Oñate, D.R.J. Owen, D. Peric and B. Suárez (Eds)

CELL-CENTERED TRUSS MODEL FOR THE ANALYSIS OF CELL RHEOLOGY AND REMODELLING

José J. Muñoz*, Nina Asadipour*, Santiago Albo*

* Laboratori de Càlcul Numèric (LaCàN), Dep. Applied Mathematics III, Universitat Politècnica de Catalunya (UPC), j.munoz@upc.edu, http://www.lacan.upc.edu/munoz

Key words: Soft tissues, active deformations, rheology, viscoelasticity, remodelling

Abstract. Soft active tissues exhibit softening, hardening, and reversible fluidisation [14]. The result of these non-linear behaviour is due to multiple processes taking part at different scales: active protein motors that actuate at the polymeric structure of the cell, (de)polymerisation and remodelling of the cytoskeleton, and cell-cell connectivity changes that take place at the tissue level.

We here present a cell-centred model that takes into account the underlying active process at the cytoskeleton level, and allows for active and passive cell-cell reorganisation and intercalation [11]. Cell-cell interactions are modelled through specific non-linear elastic laws, and coupled active deformations [12]. Cell-connectivity and cell boundaries are respectively determined with Delaunay and Voronoi diagrams of the cell-centres.

The model is compared against different experimental measures of apparent cell viscoelasticity. Passive cell reorganistation and the active cell shape changes that take during embryogenesis will be also compared against continuous models.

1 INTRODUCTION

1.1 Mechanical response of cells

Cells resident in certain hollow organs are subjected routinely to large transient stretches, including every adherent cell resident in lungs, heart, great vessels, gut, and bladder. Latest developments in non-linear cell rheology shows that the lung epithelial tissues in response to a transient stretch promptly fluidizes and then gradually resolidifies [13], but very early literature shows that in response to application of a physical force the cell acutely stiffen. The response of a living cell to transient stretch would seem to be a different matter altogether. Mechanisms of inelastic cell deformation involving stiffening and softening are reported in the literature concerning several types of both cells and

biopolymer networks [6, 9, 8, 4].

1.2 Cell viscoelasticity

It is well recognised that the cell viscosity is not solely due to the fluid part of the cytoplasm (water), but also due to the cell activity [3, 6]. However, when retrieving characteristic viscous coefficients of cells, there is wide spectrum of values that have been employed, which range from $\eta = 4.2103 Pa.s$, according to the Brownian motion of molecules in embryonic cells of Drosophila Melanogaster [7], up to $\eta = 105 Pa.s$ for cells at its wing imaginal disk, a value deduced from relaxation experiments [2, 5]. While the former values are close to water viscosity ($\eta = 8.9104 Pa.s$), the latter coefficient is in fact similar to the viscosity of olive oil or ketchup like materials. Hence, in order to shed light into the mechanisms that cause the cellular response of the cell, it seems necessary to bridge the measured viscosity and the cellular biomolecular processes.

2 ELASTIC MODEL WITH ACTIVE LENGTHENING

We propose an evolution law of the remodelling process in the cytoskeleton which is able to mimic the viscous properties of biological cellular tissues. From the physical point of view, when a set of cross-linked actin filaments in the cytoskeleton is subjected to a macroscopic strain, it stretches as a result of two combined phenomena: (i) a reversible (elastic) deformation and a (ii) non-reversible remodelling and lengthening. The latter is illustrated in Figure 1, and phenomenologically explained as the remodelling of the cross-links and a (de)polymerisation process of the filaments. In addition, we hypothesise that (iii) the current resting length L of the combined filaments, that is, the total length of the filaments when subjected to zero loads at their ends, is proportional to the elastic strain.

The previous picture may be mathematical described in a simple manner by assuming that the resting length satisfies the following evolution law:

$$\dot{L} = \gamma \varepsilon L = \gamma (l - L), \tag{1}$$

that is, the relative changes of the resting length is proportional to the current elastic strain, with l the current total length of the network. The parameter γ will be called the remodelling rate, which represents the resistance of the network to adapt its configuration to the new imposed deformation. The rheological model with active lengthening is depicted with the symbol in Figure 2.

The evolution law in (1) is implemented in conjunction with a non-linear elastic constitutive law, where the elastic force along the direction $\boldsymbol{x}_1 - \boldsymbol{x}_2$ of a two noded bar is given by,

$$\boldsymbol{g}^e = k\varepsilon \exp(-\alpha \varepsilon^2) \frac{1}{\| \boldsymbol{x}_1 - \boldsymbol{x}_2 \|} \left\{ \begin{array}{c} \boldsymbol{x}_1 - \boldsymbol{x}_2 \\ \boldsymbol{x}_2 - \boldsymbol{x}_1 \end{array} \right\} \tag{2}$$

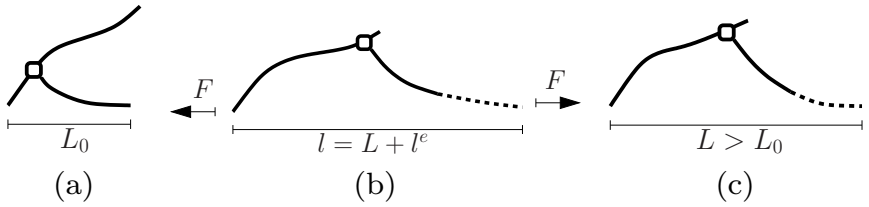

Figure 1: Schematic of strain induced changes in the resting length L of a reduced system with two filaments and a crosslink (white circle). (a) Initial configuration with resting length equal to L_0. (b) Configuration under an applied load. (c) New unstrained configuration with modified resting length $L > L_0$. Dotted lines indicate extensions of the filament due to filament polymerisation.

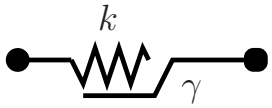

Figure 2: Elastic rheological model with active lengthening.

with $\varepsilon = \frac{l-L}{L}$ the elastic strain, and α a material parameter the measures the softening of the material. For $\alpha = 0$, linear elastic behaviour is recovered.

2.1 Mode-dependent softening

The reversible softening process observed in lung epithelial tissues [13], where the tissues softens and decreases the phase angle after a sudden stretch, and eventually recovers its initial properties (see Figure 7a). Such softening has been reproduced with a viscoelastic constitutive in [11]. In order to reproduce the eventual recovery of the initial elastic properties, we will apply elastic element with active lengthening with an non-symmetric factor which has different values depending on the sign of the elastic strain ε^e. More specifically, given a nominal value γ_0, we apply the following remodelling rate γ:

$$\gamma = \begin{cases} \gamma = \gamma_0, & \text{if } \varepsilon^e \geq 0 \\ \gamma = r_\gamma \gamma_0 & \text{if } \varepsilon^e < 0 \end{cases}$$

where r_γ is the reduction parameter. Physically, r_γ corresponds to the difference between the polymerisation and the de-polymerisation time which allows to simulate recovery of stiffness.

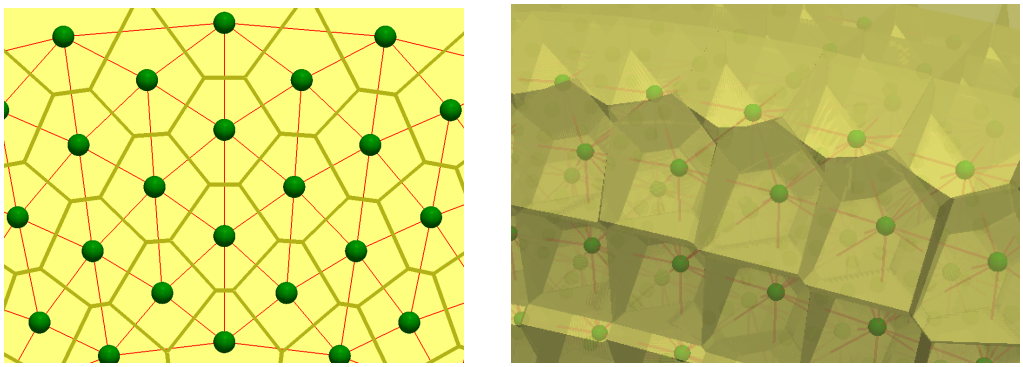

(a) (b)

Figure 3: Scheme of the cell-centered model: spheres represent cell nucleai, thin lines cell-cell contacts, and thick lines (a) and opaque faces (b) depicture the cell boundaries. All forces between neighbouring cells are represented by a single truss element, which is constructed by using a Delaunay trinagularisation of the cell-nucleai. The cell boundary corresponds to the Voronoi diagram of the triangularisation.

3 CELL-CENTERED MODEL FOR MULTICELLULAR SYSTEMS

From endocytosis to crawling motility, a vast array of cellular functions requires the cytoskeleton to organize and remodel the intracellular space and surrounding membranes. In order to represent the reorganization (remodeling) of the cytoskeleton, we extended the cell-centered model of tissues, where each node represents the cell nucleus, and each truss carries the intra- and intercellular forces between two adjacent cells Fig (3). In this model, all considered physical properties of the cells can be described by the cell centers relative configuration. We also add the corresponding Voronoi diagram, which illustrate the cell boundary. This boundary is determined in the post processing of the Delaunay triangulation, but so far does not carry any mechanical force.

3.1 Delaunay triangulation

A Delaunay triangulation of a set P of points, $DT(P)$, in a plane is such that no point in P is inside the circumcircle of any triangle in $DT(P)$. This approach minimizes the angles of the triangles in the triangulation; in simple terms this ensures no skinny triangles are created. Delaunay triangulation has been implemented as the topological pattern to generate Finite Element meshes, i.e. providing the connectivity between centers of every two neighboring cells.

In our model, a Delaunya triangularisation is implemented on each new configuration of the cells aggregate in equilibrium, obtained after each increment of applied force/displacement. Figure 4 illustrates a schematic view of Delaunay triangulation, being recovered for a set of four nodes (cell centers) , after yielding a new configuration in equilibrium.

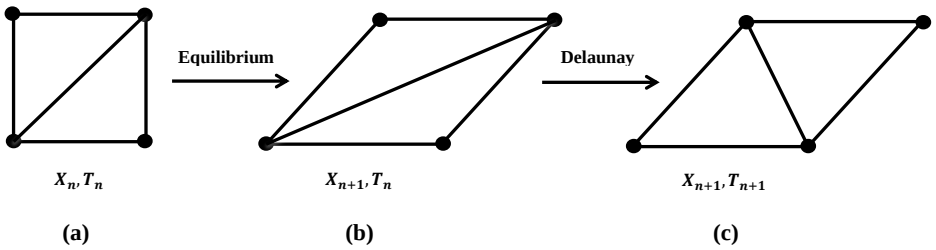

Figure 4: A schematic view of Delaunay triangulation for a set of four nodes: a) primary Delaunay triangulation. b) new configuration in equilibrium. c) recovering Delaunay triangulation for the new configuration.

One of the properties of the Delaunay's algorithm is that the union of all the simplexes of the triangulation yields the convex hull of the points. Therefore, a basic Delaunay triangulation of a set of cell centers may invariably lead to distant boundary cells being unrealistically connected, i.e. covering non-convex boundaries.

In order to overcome this problem, those elements with very high aspect ratio were eliminated by defining a filtering process. The ratio of in-radius to circum-radius of each triangle in 2D problem and each tetrahedral in 3D problem has been considered as an appropriate criterion to filter undesirable simplexes.

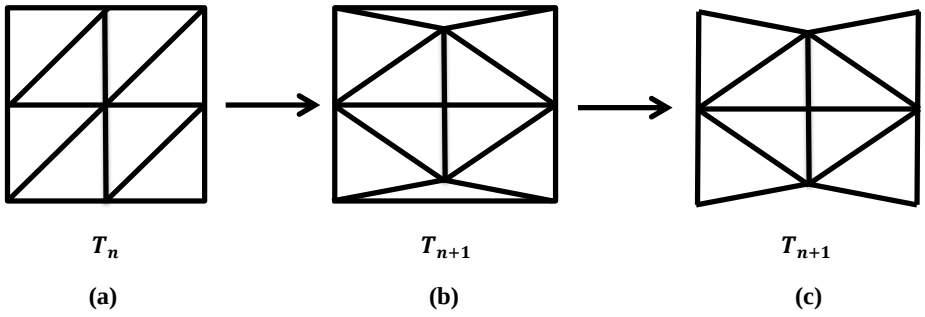

Figure 5: Filtering process of Delaunay triangulation: a) primary configuration with Delaunay triangulation, b) new configuration in equilibrium while presence of unrealistic connectivities, c) unrealistic connectivities being filtered.

Therefore, after applying the filtering condition to the Delaunay triangulation implemented at each obtained configuration, the unrealistic elements on the boundary were removed from the connectivity matrix. Figure 5 shows a schematic view of a set of nodes in a 2D plane, in a matrix obtained by Delaunay triangulation while being filtered, after yielding a configuration in equilibrium.

3.2 Voronoi tessellation

Voronoi tessellation is a method to represent the boundaries of cells, in contact with each other in a cell aggregate. It is constructed with respect to the connectivity matrix obtained by Delaunay triangulation, where each Voronoi face splits in half the connecting line between centres of every two neighbouring cells.

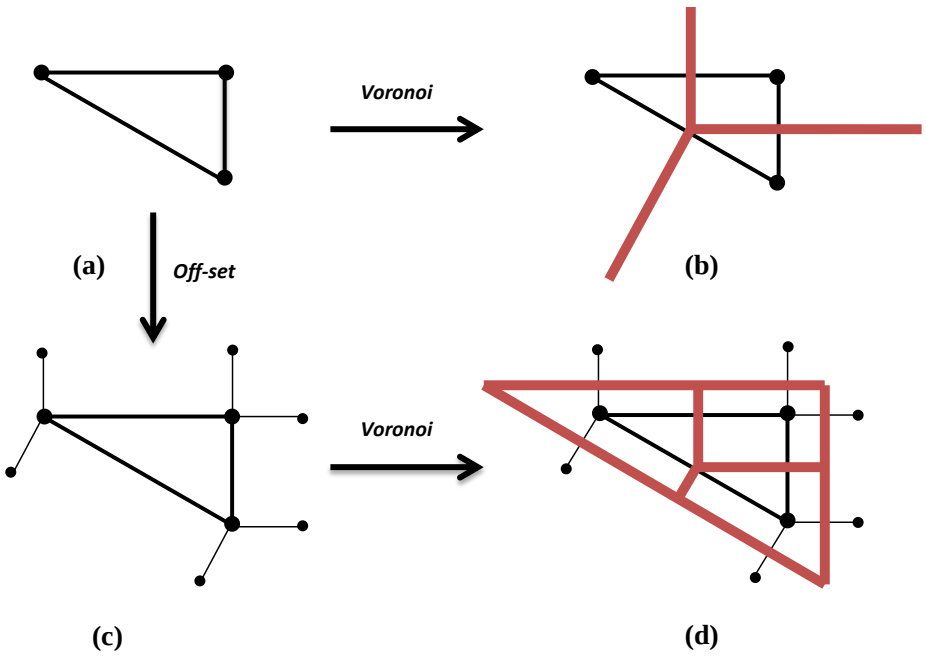

Figure 6: Voronoi tessellation: a) Delaunay triangulation of original set of nodes, b) voronoi tessellation

However, when it comes to construct the boundaries associated with the cells at the surface of the cells aggregate, Voronoi faces form unbounded regions when two consequent Delaunay vertices on the surface, form a convex configuration. To resolve this issue, a set of off-set nodes were added to the original set where each was constructed at a fixed distance to every original node at the surface, perpendicular to each of vertices the node associated to. As a result, for every surface node there was the same number of off-set nodes constructed as the vertices it associated to. Then a new Voronoi tessellation was constructed over the original and off-set nodes, promising the formation of bounded regions for the original nodes at the surface. Figure 6 illustrates a schematic view of a set of three nodes primarily connected by Delaunay triangulation. Then a Voronoi tessellation led to unbounded regions, while considering off-set nodes guaranteed Voronoi tessellation yielding bounded regions for original nodes.

4 COMPARISON OF MAXWELL AND ACTIVE MODEL

Next, we will compare the response of the Active model (elastic element with active lengthening) with a linear elastic Maxwell model to a sudden stretch (stress relaxation) and a constant load (creep). In these two cases, a single one-dimensional element with initial length L_0 and prescribed displacement at the right end, was used.

It can be shown that by comparing the analytical solutions of these tests, that the Maxwell element and the active element have a very similar reponse if the parameter γ is replaced by τ^-1. Furthermore, after applying a cycling load, and at small strains, it can be deduced that the dependence of the phase angle $\delta = \text{atan}\frac{G''}{G'}$ with respect to ω follows the relation given in Table 1, with G'' and G' the loss and the storage modulus. The results on the table confirm the equivalence between the parameter γ and the ratio η/k, as also experimentally confirmed in [10, 1].

	G'	G''	$\tan\delta$
Maxwell	$\frac{k\eta^2\omega^2}{k^2+\eta^2\omega^2}$	$\frac{k^2\eta\omega}{k^2+\eta^2\omega^2}$	$\frac{k}{eta}\omega^{-1}$
Active	$\frac{k\omega^2}{\omega^2+\gamma^2}$	$\frac{k\gamma\omega}{\omega^2+\gamma^2}$	$\gamma\omega^{-1}$

Table 1: Phase angle $\delta = \text{atan}\frac{G''}{G'}$ as a function of the frequency ω for the Maxwell and Active model.

These results show that the remodelling process can be identified with the viscous properties of the cell. In the next section we show that the extension of the model given in Section 2.1 allows to further match the softening behaviour.

5 MODELLING OF SOFTENING

In 2007, Xavier Trepat and his group demonstrated that a living cell promptly fluidizes and then slowly re-solidifies under stretch[13]. They subject the adherent human airway smooth muscle (HASM) cell to a transient isotropic biaxial stretch-unstretch manoeuvre. They could then monitor, on the nanometre scale, cell mechanical properties, remodelling dynamics and their changes. Stiffness after stretch relative to stiffness of the same cell immediately before was denoted G'_n. As shown in Figure (7,a), when no stretch was applied, this fractional stiffness did not change, but immediately after cessation of a single transient stretch, G'_n promptly decreased while the phase angle $\delta = tan^{-1}(G''/G')$ increased and then both recovered slowly.

In order to obtain the mentioned characteristics of the living cells, we have implemented the elastic active element described in Section 2 for one truss element. We have successfully simulated the fluidisation process of the cell by controlling different rates of

lengthening during tension and compression (Figure 7,b).

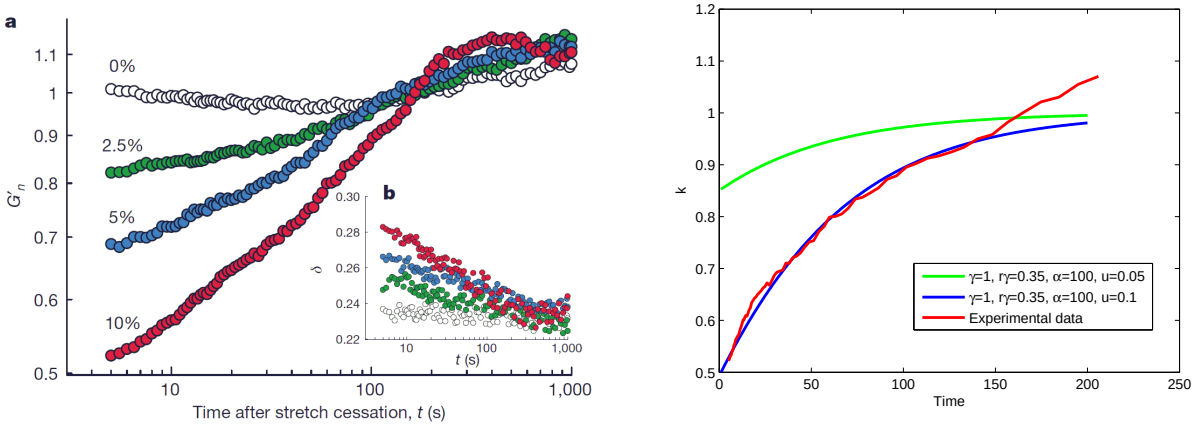

(a) (b)

Figure 7: a) A single transient stretch drives fractional stiffness G'_n down and the phase angle δ up, indicating fluidization of the cytoskeleton.**a**, Evolution of G'_n of HASM cells after a single transient stretch of 0%, 2.5% (green), 5% (blue) and 10% (red). **b**, Evolution of the phase angle after stretch application. b) The value of the effective stiffness $k = k_0 \exp(-\alpha\varepsilon^2)(1 - 2\alpha\varepsilon^2)$ of the elastic element with active lengthening model.

6 CONCLUSIONS

In this work we have proposed an evolution law of the macroscopic remodelling process which mimics the apparent measured viscosity. The proposed law in Equation (1) aims to (i) reproduce the ability of the cell to adapt to the current strains, and (ii) respond with a limited amount of sustained stress. Despite its simplicity, this evolution law is able to reproduce the viscoelastic response at small strains. The resting length changes have been combined with a purely linear elastic law, and the resulting active model has been compared against a linear Maxwell model. The model was developed to simulate global actin-network dynamics in soft tissues but can be equally applied to other engineering problems, and may be easily extended to include other non-linear effects such as incompressibility constraints or growth.

Also, we have applied the methodology to model reversible stiffness softening a nonlinear elastic and viscous behaviour that has been experimentally observed in biomechanical tests performed on epithelial lung cell monolayers [13].

7 ACKNOWLEDGMENTS

The authors acknowledge the International Association of Computational Mechanics (IACM) for their participation scholarship to the World Congress on Computational Me-

chanics (ECCM 2014).

REFERENCES

[1] D Azevedo, M Antunes, S Prag, X Ma, U Hacker, GW Brodland, M S Hutson, J Solon, and A Jacinto. DRhoGEF2 Regulates Cellular Tension and Cell Pulsations in the Amnioserosa during Drosophila Dorsal Closure. PLOS ONE, 6(9):e23964, 2011.

[2] T Bittig, O Wartlick, A Kicheva, M Gonzalez, and F Juliher. Dynamics of anisotropic tissue growth. New J. Phys.063001, 2008.

[3] A Besser, J Colombelli, EHK Stelzer, and U S Schwarz. Viscoelastic response of contractile filament bundles. Phys. Rev.051902, 2011.

[4] Chaudhuri, O., Parekh, S., Fletcher, D., 2007. Reversible stress softening of actin networks. Nature 445, 295-298.

[5] G Forgacs and RA Foty and Y Shafrir and MS Steinberg. Viscoelastic properties of living embryonic tissues, 1998.

[6] Y. C. Fung, Biomechanics : mechanical properties of living tissues, 2nd Edition, Springer, New York, 1993.

[7] T Gregor, W Bialek, RR de Ruyter van Steveninck, DW Tank, and E F Wieschaus. Diffusion and scaling during early embryonic pattern formation. Proc. Nat. Acad. Sci. USA, 20:184031407, 2005.

[8] Janmey, P. A., Euteneuer, U., Traub, P., Schliwa, M., 1991. Viscoelastic properties of vimentin compared with other filamentous biopolymer networks. J. Cell Biol. 113 (20), 155-160.

[9] Krishnan, R., Park, C. Y., Lin, Y. C., Mead, J., Jaspers, R. T., Trepat, X., Lenormand, G., Tambe, D., Smolensky, A. V., Knoll, A. H., Butler, J. P., Fredberg, J. J., 2009. Reinforcement versus uidization in cytoskeletal mechanoresponsiveness. PLOS ONE 4, e5486.

[10] X Ma, H E Lynch, P C Scully, and M S Hutson. Probing embryonic tissue mechanics with laser hole drilling. Phys. Biol., 96:036004, 2009.

[11] J. J, Muñoz, V. Conte, N. Asadipour and M. Miodownik. A truss element for modelling reversible softening in living tissues. *Mech. Res. Comm.*, Vol. **49**, 44-49, 2013

[12] J. J, Muñoz and S. Albo. Physiology-based model of cell viscoelasticity. *Phys. Rev. E*, Vol. **88**, 012708, 2013.

[13] X. Trepat, L. Deng, S. An, D. Navajas, D. Tschumperlin, W. Gerthoffer, J. Butler, J. Fredberg, Universal physical responses to stretch in the living cell, Nature 447 (3) (2007) 592596.

[14] L. Wolff, P. Fernández and K. Kroy. Resolving the Stiffening-Softening Paradox in Cell Mechanics, Vol. **7**, e40063, 2012.